JP 4.6 ON THE EXCESS MIXING IN NWP MODELS IN STABLE BOUNDARY LAYERS: THE POSSIBLE ROLE OF OROGRAPHIC GENERATED SUB-GRID GRAVITY WAVE DRAG

G.J. Steeneveld[*1], A.A.M. Holtslag[1], C.J. Nappo[2] and L. Mahrt[3]

[1]Wageningen University, Wageningen, The Netherlands
[2]Air Resources Laboratory, Atmospheric Turbulence and Diffusion Laboratory, NOAA, Oak Ridge, U.S.A.
[3]College of Oceanic & Atmospheric Sciences, Oregon State University, Corvallis, OR, U.S.A.

1. INTRODUCTION

The atmospheric boundary layer (ABL) is a turbulent layer that feels the impact of the surface on a timescale of one hour or less. Our ability to model the ABL on a large spatial scale during stable stratification is rather poor at the moment (Holtslag, 2003). Contrary, Steeneveld et al. (2006) showed good model results on a local scale using detailed knowledge of the local surface characteristics and the large-scale forcing. The main difference between the large-scale and the local approach is the larger amount of friction/ turbulent mixing (τ_{turb}) in large-scale models. This is necessary to maintain good skill scores (Beljaars and Viterbo, 1998), although this "enhanced mixing" cannot be justified from local observations (amongst others Businger et al., 1971) and Large-Eddy Simulation (Beare et al., 2006). The objective of this paper is to investigate the possible role of gravity wave drag on the total drag in the stable boundary layer (SBL).

2. THEORY

The momentum flux-profile relationship from LES and observations for the SBL reads (Monin-Obukhov Similarity theory (MOS)):

$$\varphi_m = \frac{kz}{\sqrt{\tau_{turb}}}\frac{\partial U}{\partial z} = 1 + 5\frac{z}{L}, \qquad (1)$$

or equivalent

$$F_m = \varphi_m^{-2} = \left(1 - 5Ri_g\right)^2 \qquad (2)$$

with *L* the Obukhov length and *z* the height above the surface. *U* is the mean wind speed, Ri_g the gradient Richardson number and *k* the Von Karman constant. Figure 1 depicts Equation (2), together with the F_m-formulation in the current ECMWF model. It is clear that the two functions do not match. The consequence of the excess mixing in the ECMWF model is a deterioration of the boundary-layer structure, which should be avoided.

Although the functional form of φ_m vs *z/L* Equation (1) appears to be consistently found both from several observational datasets (e.g. Beljaars and Holtslag, 1991) and from LES, we assume in this approach that the total amount of friction in the boundary layer is through turbulent drag. The persistent difference shown in Figure 1 may indicate that we miss a certain process in the drag parameterization, in addition to turbulent drag.

An important property of a stably stratified flow is the ability to propagate gravity waves. Small-scale orography generates upward propagating gravity waves, with an amount of stress τ_{wave}. At a certain level where the wind speed vanishes, the gravity wave meets a critical level where the wave dissipates nearly totally. Consequently, a divergence of the gravity wave drag occurs. Note that the divergence of wave stress will always act against the flow. It is always a negative acceleration. This mechanism is the same as for large mountain ridges. However, the SBL is shallow, and thus also small-scale orography can have a significant impact on the flow in the SBL through gravity wave propagation. Nappo (2002) and Chimonas and Nappo (1989) showed that this wave drag compared to turbulent drag during weak winds.

The reason these gravity waves may not be seen in regular turbulence observations is because the wave are standing waves and perturbations are thus not seen when you observe at a single location.

An additional argument for this approach with gravity wave drag lies in the fact that SBL parameterizations have been derived for idealized flat terrain (e.g. Cabauw, The Netherlands). Contrary to that, the majority of the landscapes is not flat terrain.

[*]*Corresponding author address*: G.J. Steeneveld, Wageningen University, Meteorology and Air Quality Group, Duivendaal 2, 6701 AP Wageningen, The Netherlands. E-mail: Gert-Jan.Steeneveld@wur.nl

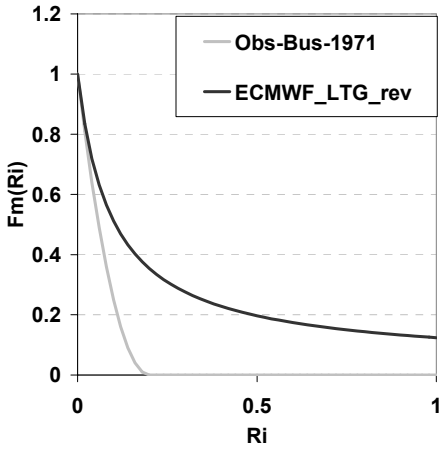

Figure 1: The turbulent mixing F_m as function of stability from observations (grey line) and in the ECMWF model (black line).

In the linear theory, the gravity wave drag for an (idealized) surface corrugation is given by (Nappo, 2002):

$$\tau_{wave} = \begin{cases} 0.5\rho_0 k_s (u_0 H)^2 \sqrt{\frac{N^2}{u_0^2} - k_s^2} \;\; .....for \; \frac{N}{u_0} > k_s \\ 0 \;\; .....for \; \frac{N}{u_0} \le k_s \end{cases} \quad (3)$$

which for small wind speed reduces to:

$$\tau_{wave} = 0.5\rho_0 k_s N H^2 u_0 \quad (4)$$

with N the Brunt-Vaisaila frequency, H and k_s the amplitude and the wave number of the orography respectively, and ρ_0 the air density and u_0 the background wind speed.

To examine the impact of gravity wave drag on the flux-profile relationship (1), we define an apparent dimensionless wind speed gradient (in which gravity wave drag is added to turbulent drag) φ_m^*:

$$\varphi_m^* = \frac{kz}{\sqrt{(\tau_{turb} + \tau_{wave})\rho^{-1}}} \frac{\partial U}{\partial z} \quad (5)$$

and investigate its relationship with Ri_g.

3. OBSERVATIONS

We use CASES-99 observations, taken October 1-31, 1999 near Leon, Kansas, U.S.A. (37.6486º N, -96.7351º E, 430 m a.s.l. especially to study the relevant processes in the SBL (Poulos et al., 2002). The area is a relatively flat (on a local scale) prairie grassland and free of obstacles. On a larger scale, some minor topography is present with a wavelength of L_x = 1600 m and an amplitude of H =15 m (Figure 2). Note that H/L_X is only of order 1%.

The relevant observations exist of wind speed profiles and turbulent fluxes. Surface turbulent momentum (u_*) is obtained with the eddy covariance technique at 2.6 m and temperature at the mast by thermocouples (10 minutes averages).

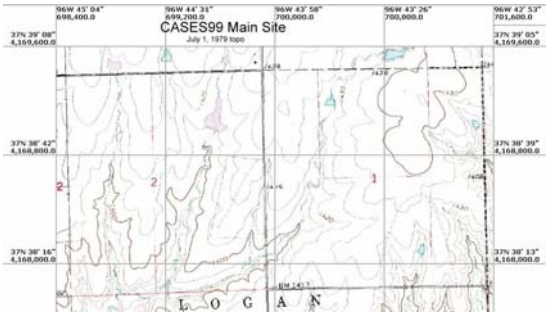

Figure 2: CASES-99 topography.

4. RESULTS

We stratify our data according to N/u_0, which is in fact equivalent to the Froude number. We only selected data with a mean wind speed less than 5 ms^{-1}. N and u_0 are calculated as the averaged wind speed and stratification in the layer between 15 and 55 m. This is of course a rough estimate, but sufficient to make a reasonable first order estimate for u_0 and N.

We will plot F_m vs Ri_g, although we know that this scaling is inappropriate, since turbulence should be scaled with Eq. (1) and wave stress with Eq. (3). However, to compare the combined effect of turbulent and wavedrag on the wind speed profile and compare with the formulation in ECMWF, we adopt Eq. (5). Figure 3 shows that for the class $0.010 < N/u_0 < 0.015$, the data with turbulence only shows $F_m \rightarrow 0$, following MOS. When we include the gravity wave drag (calculated with (4)), F_m is increased significantly for $0.2<Ri_g<0.3$. The scatter is large, but not unreasonable in the field of boundary-layer meteorology. For $Ri_g > 0.6$, the data with wave drag included seems to follow the F_m function in the ECMWF model.

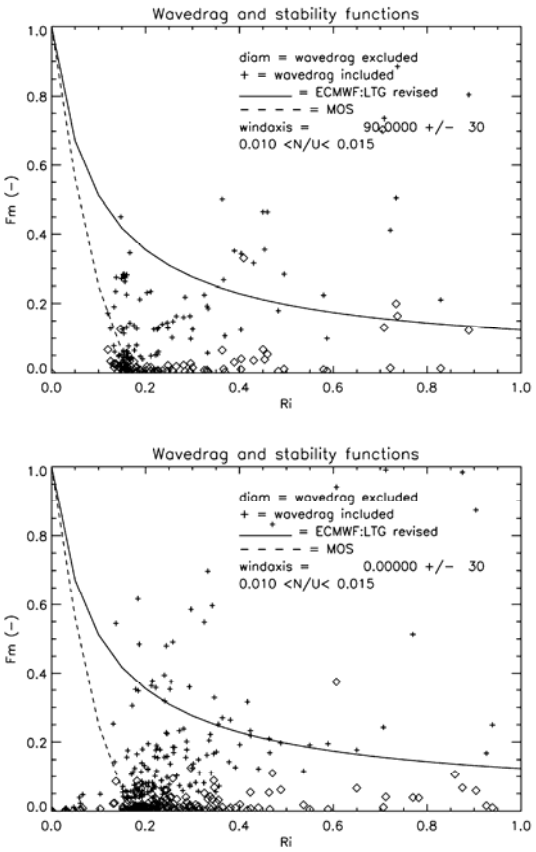

Figure 3: Stability function F_m as function of Ri_g for class $0.01<N/u_0<0.015$ and north-south direction (a) and east-west-direction (b). Diamonds: only turbulent drag included (not plotted for $Ri_g<0.15$), +: both turbulent and wave drag included, Full line: ECWMF mixing function; Dashed line: local observations.

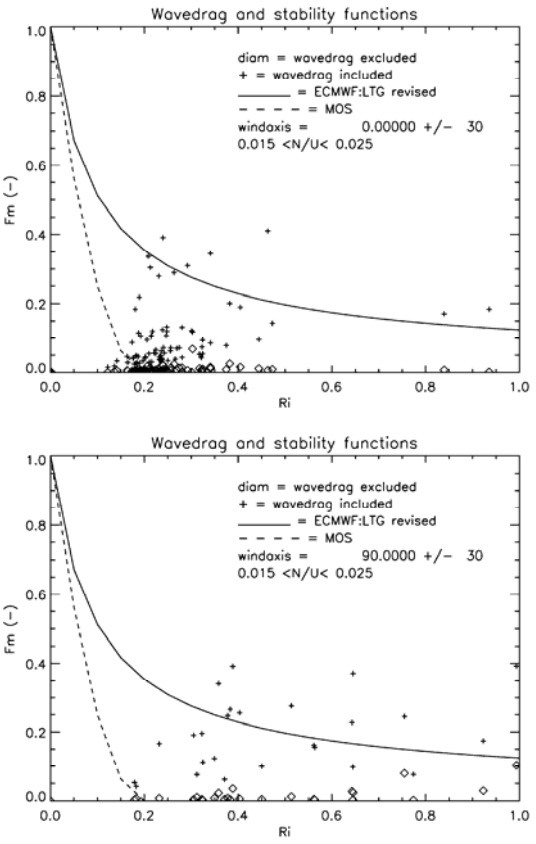

Figure 4: As Figure 3, but for $0.015 < N/u_0 < 0.025$.

Figure 4 shows similar results for $0.015 < N/u_0 < 0.025$. Similar results are found as in Fig. 3, but the correspondence between the "long tail" and wave drag included data is even more evident.

Finally, we have to realize that the model line in the ECMWF is thus not unique but in reality depends on the stratification and the wind speed in the grid cell.

5. DISCUSSION

The concept proposed in this paper might oversimplify the concept of gravity wave drag in the SBL since we do not try to model the effect of each individual gravity wave, but the impact of gravity waves on the total drag on a large scale.

In addition to these gravity waves generated by the local topography, gravity waves generated by roughness changes and convective systems are not considered here, but may have their impact as well.

Furthermore, we should be aware that a constant N and u_0 is an oversimplification of the ABL structure during nighttime. In reality u_0 and N increases both nonlinearly with height, so wave reflections may occur in reality, which is not accounted for in the current formulation.

We remark that orography also give additional drag if gravity waves are absent. In this case the turbulent drag and the pressure force over the orography is enhanced. Brown and Wood (2003) conclude that these effects can be well described by an effective roughness length in the turbulence parameterization.

An additional impact is the direction of the total stress vector. With turbulence only, the stress is aligned parallel to the shear. However, for orographic generated gravity waves, the stress is aligned perpendicular to the mountain ridge and not to the wind speed vector. The rotation of the stress vector (as function of stability) has been a recent topic in many NWP models, e.g. HIRLAM (Sass and Woetmann-Nielsen, 2005).

Finally, we would like to remark that our results are rather tentative and should be validated against more data sets, and tested with LES and also mesoscale models.

6. CONCLUSIONS

We propose a concept that subgrid gravity wave drag is an important and significant part of the drag in the stable boundary layer, in addition to the turbulent drag. Using first order estimates of this gravity wave drag, we find good agreement between observed total drag and the total drag needed in a Numerical Weather Prediction model. As such, the gravity wave drag may act as the bridge between "short tail" and "long tail" mixing functions. Splitting the total drag in a turbulent and non-turbulent part will give sufficient drag without deteriorating the boundary layer structure in a large-scale weather prediction model.

REFERENCES

Beare, R.J., and co-authors, 2006: An intercomparison of Large-Eddy Simulations of the stable boundary layer, *Boundary-Layer Meteorol,* in press.

Beljaars, A.C.M and A.A.M. Holtslag, 1991: Flux parameterization over land surfaces for atmospheric models, *J. Appl. Meteo*rol, **30**, 327-341.

Beljaars, A.C.M. and P. Viterbo, 1998: Role of the boundary layer in a numerical weather prediction model, in *Clear and Cloudy boundary layers*, A.A.M. Holtslag and P.G. Duynkerke Eds, Royal Netherlands Academy of Arts and Sciences, Amsterdam, 372pp.

Brown, A.R, and N. Wood, 2003: Properties and Parameterization of the Stable Boundary Layer over Moderate Topography, *J. Atmos. Sci*, **60**, 2797-2808.

Businger, J.A., J.C. Wyngaard, Y. Izumi and E.F. Bradley, 1971: Flux profile Relationships in the Atmospheric Surface Layer, *J. Atmos. Sci*, **28**, 181-189.

Chimonas, G. and C.J. Nappo, 1989: Wave drag in the planetary boundary layer over complex terrain, *Bound.-Layer Meteor.*, **47**, 217-232.

Holtslag, 2003: GABLS initiates intercomparison for stable boundary layer case, *GEWEX newsletter*, **13**, 7-8.

Nappo, C.J., 2002: An Introduction to Atmospheric Gravity Waves, Academic Press, London, 276 pp.

Poulos, G.S., and co-authors, 2002: CASES-99: A comprehensive Investigation of the stable nocturnal boundary layer, *Bull. Am. Met. Soc.*, **83**, 555-581.

Sass, B, and N. Woetmann-Nielsen, 2005: Modelling of the HIRLAM surface stress direction, *HIRLAM Newsletter*, **45**, 8pp.

Steeneveld, G.J., B.J.H. van de Wiel and A.A.M. Holtslag, 2006: Modeling the evolution of the atmospheric boundary layer for three contrasting nights in CASES-99, *J. Atmos. Sci.*, **63**, 920-935.